Parametric Uncertainty Analysis of a Hall Thruster through a Fully Kinetic Code

IEPC-2015-255／ISTS-2015-b-255

Burak KARADAG[1]
The Graduate University for Advanced Studies (SOKENDAI), Japan

and

Shinatora CHO[2], Ikkoh FUNAKI[3]
Japan Aerospace Exploration Agency, Japan

For better prediction accuracy of fully kinetic particle Hall thruster simulation, a systematic one-at-a-time sensitivity analysis of model uncertainties was presented. The sensitivity of model input parameters to thrust performance was investigated to evaluate the effects of thermal accommodation coefficient, anode/wall temperature, Bohm diffusion coefficient, electron injection current, cathode coupling voltage, and background pressure. The simulation was conducted on a laboratory model magnetic layer type Hall thruster, and the impact of each source of uncertainty on the simulation result was quantified. The results show an overall confidence range of +15%-16% for thrust and +14%-19% for discharge current relative to the model parameter uncertainties. Among the sources of uncertainties, the Bohm diffusion coefficient and the uncertainties related to the neutral flow (thermal accommodation coefficient and anode/wall temperature) were found to be dominant over other uncertainties. Although this study was the preliminary step toward the uncertainty quantification of fully kinetic Hall thruster modeling, it was found that uncertainties related to the neutral flow showed significant impacts on performance evaluation of Hall thruster, and the neutral flow effect was found to be comparable to the effects of Bohm diffusion coefficient despite of the less attention they attracted so far.

Nomenclature

A	=	thermal accommodation coefficient & anode/wall temperature
ALL	=	overall uncertainty
B	=	Bohm diffusion coefficient
BP	=	background pressure effect
C	=	cathode coupling voltage
E	=	electron injection current
E_{co}	=	thermal accommodation coefficient for ions
F	=	thrust
I_b	=	beam current
I_{b1}	=	singly charged ion current
I_{b2}	=	doubly charged ion current
I_d	=	discharge current
I_n	=	neutral current
K_B	=	Boltzmann constant

[1] Graduate Student, Department of Space and Astronautical Science, 3-1 -1 Yoshinodai, Chuo-ku, Sagamihara, Kanagawa 252-5210 Japan
[2] Researcher, Institute of Aeronautical Technology, 7-44-1 Jindaiji, Higashi-machi, Chofu-shi, Tokyo, Japan
[3] Associate Professor, Department of Space Flight System, 3-1 -1 Yoshinodai, Chuo-ku, Sagamihara, Kanagawa 252-5210 Japan

M	=	ion mass
$\dot{m}$	=	anode mass flow rate
max	=	maximum
min	=	minimum
nom	=	nominal
q	=	the unit charge
Q	=	average ion charge
P_d	=	discharge power
P_{jet}	=	jet power
T	=	temperature
T_{anode}	=	anode temperature
T_{co}	=	thermal accommodation coefficient for neutrals
T_{wall}	=	inner and outer wall temperature
V_b	=	average beam potential
V_c	=	cathode coupling voltage
V_d	=	discharge voltage
ω_c	=	electron plasma frequency
y_0	=	normalized speed ratio for neutrals
τ	=	average collision time
Δ	=	discharge current oscillation amplitude
η_A	=	anode efficiency
η_E	=	energy efficiency
η_V	=	voltage utilization efficiency
η_C	=	current utilization efficiency
Φ_P	=	propellant efficiency
Φ_q	=	charge utilization efficiency
Φ_m	=	mass utilization efficiency
$\Phi_{N\text{-}G}$	=	neutral-gain utilization efficiency
Ψ_B	=	beam efficiency
$\langle\overline{v^2}\rangle_m$	=	mass weighted average of square of velocity
$\langle\overline{v}\rangle_m$	=	mass weighted average velocity
$\langle\overline{v_i}\rangle_m$	=	mass weighted average ion velocity
$\langle\overline{v_i{}^2}\rangle_m$	=	mass weighted average of square of ion velocity

I. Introduction

A Hall thruster[1] is a type of electric propulsion used for satellite missions like station keeping, orbit transfer or deep space exploration. Hall thrusters are usually classified into two major types: Magnetic layer type (SPT) Hall thrusters, which has a dielectric ceramic discharge channel wall, usually Boron Nitride (BN); Anode layer type (TAL) Hall thruster, which has a metallic channel wall biased to cathode potential to minimize the electron wall loss. SPTs are the most developed and the most used Hall thrusters for satellite missions because of their reliability. In a Hall thruster, electrons are injected into a radial magnetic field by the cathode. Magnitude of the magnetic field (100-200 Gauss) is strong enough to trap the electrons and insert them into spiral orbit around the magnetic field lines inside the chamber due to the $\boldsymbol{E}\times\boldsymbol{B}$ drift. Hall current, which enables the heavy particle acceleration and thrust generation, is formed by this azimuthal guiding center drift. The entrapped electrons, which ionize the neutral propellant, are gradually accelerated toward the anode and a strong axial electric field is maintained throughout the discharge channel. The ions are too heavy to be affected by the magnetic field. Therefore, they are accelerated by the axial electric field, exhausted in high speed generating thrust according to Lorentz force, and finally neutralized by electrons emitted from the cathode not to charge the spacecraft.

Hall thrusters are preferable due to many advantages such as high thrust density (No space-charge limitation defined by Child's law as ions are accelerated in quasi-neutral plasma), moderate specific impulse, and outstanding in-space experience. However, state of the art Hall thrusters have an efficiency of 60% with specific impulses in the range of 1500–3000s, and increasing demand for space missions requires Hall thrusters with better performance and lifetime. To improve/optimize performance of Hall thrusters and understand discharge chamber plasma physics, numerical simulations are important in that they are cheaper and faster compared to experiments and they provide physical information often difficult to obtain from experiments. For example, quantifying plasma properties inside the discharge chamber is a difficult task as interaction of probes with highly energetic particles would affect the measurement result. For the present, numerical simulations are only assistive methods and unlikely to replace the experiment since complex plasma behavior is far from being well understood.

There are three main approaches (Fluid, fully kinetic, and hybrid) in modeling Hall thrusters. Fluid codes treat both electrons and ions as fluid and assumes Maxwellian velocity distribution function (VDF).[2] Fully kinetic codes, treats electrons and ions as discrete particles and compute VDF self-consistently.[3] As for hybrid codes, electrons are treated as fluid whereas ions are treated as particles compromising between fluid and kinetic approaches.[4, 5] Fully kinetic codes are computationally expensive and time-consuming; however, they can capture non-equilibrium features unlike the fluid and hybrid codes. For instance, plasma-wall interaction, so-called sheath, is self-consistently modeled in fully kinetic codes, while a sheath model is used in fluid and hybrid codes. It is therefore expected that fully kinetic simulation is potentially capable of highly-accurate performance prediction for Hall thrusters. Nevertheless, there are still various sources of uncertainty involving both numerical discretization errors and model parameter uncertainties such as wall temperature in fully kinetic codes, which can degrade the prediction accuracy of the simulation. It is hence necessary to investigate these errors and uncertainties and quantify its confidence range for the realization of predictive modeling; however, so far, there was few studies tackled on this challenge, in particular for the model parameter uncertainties of fully kinetic simulation. Therefore, this study serves as the first step of uncertainty quantification of fully kinetic Hall thruster modeling by systematic one-at-a-time sensitivity analysis of model parameter inputs.

The model parameters investigated in this study includes thermal accommodation coefficient of heavy particles, anode temperature, wall temperature, Bohm diffusion coefficient, cathode coupling potential drop, electron injection current to the computational domain, and background pressure effect. This set of parameters essentially comprises all of the model parameters of fully kinetic simulation, and each of them can have non-trivial influence on the simulation result: Thermal accommodation coefficient and anode/wall temperature are expected to change the neutral flow inside the discharge channel;[6] The noble Bohm diffusion coefficient is known to be dominating the electron cross-field transport;[7] Cathode potential drop and electron injection current are related to the thruster-cathode coupling which can mainly influence the voltage utilization of ions;[8] And background pressure effect[9] is attracting increasing attention from the Hall thrusters community[10] though it is an uncertainty of experiment rather than simulation. All of these uncertainties can be categorized into epistemic uncertainty[11] or systematic error, which means there is a true deterministic value for each parameter though we do not know about its exact value due to lack of accessibility(i.e. unable to measure, measurement error, etc.). Therefore, we treated this parameters simply by a presumed confidence range, and conducted sensitivity analysis assuming the monotonicity of the response of the simulation result. In this study, a laboratory model magnetic layer type Hall thruster of the University of Tokyo with outer channel diameter of 62 mm named UT-62 was chosen to be the test bed. The simulation result of sensitivity analysis was presented in the paper and the importance of the model parameters was discussed.

II. Numerical Methodology

A. Overview

The simulation model used in this study is called as 2D3V fully kinetic Particle-in-Cell (PIC)/Direct Simulation Monte Carlo (DSMC). To compensate for the reduced electron mobility across the magnetic field, an empirical Bohm diffusion coefficient is applied. In order to make simulations possible, so-called macro-particles (or super-particles) and an artificial mass ratio are used to speed up the calculations. Each macro particle represents a predefined number of real particles (ions, electrons, and neutrals). The magnetic field induced by the plasma is considered to be negligible. The magnetic field is calculated by free software abbreviated as FEMM (Finite Element Method Magnetics).

A semi-implicit field solver is used as the field solver. The electric permittivity ε is not always equal to the vacuum permittivity because the field inside the insulator channel wall is also included into the calculation domain. Space potential φ is calculated according to the Poisson's equation. To calculate particle trajectories of all species the Lorentz force equation of motion is solved by using the 4th order Runge-Kutta method. Electric and magnetic forces are applied via the PIC method while inter-particle collisions were implemented by the DSMC method. Only ions, doubly charged ions, electrons, and neutrals are simulated.

Potential difference between anode and plasma at the thruster exit boundary is set at a predefined number. The computational time-step is chosen such that the electron cyclotron motion will be captured. Uniform rectangular grid in cylindrical coordinate system (r, z, θ) is adopted, and the cell interval is arranged in the same order of the

Debye length to resolve the dielectric wall sheath. The entire code is parallelized by using MPI and PETSc, and simulations are conducted by a quad-core 3.4 GHz CPU personal computer. The further details of the simulation methodology can be found elsewhere.[12, 13]

B. Simulation Conditions

Discharge voltage, mass flow rate, and coil current were set to 300 V, 1 A_{eq} (1.361 mg/s for Xenon), and 2 Ampere respectively. Magnetic flux density for 2 Ampere coil current varies between 0.005 - 0.03 Tesla along the discharge channel centerline and its strength increases from the anode toward the thruster exit. Simulations for each case were run for 0.4 million steps. All the performance results and plasma distribution plots are time-averaged. Table 1 lists simulation nominal input parameters.

Table 1. Simulation condition.

Thruster operation condition	Discharge voltage [V]	300
	Xenon mass flow rate [mg/s]	1.36
	Magnetic coil current [A]	2.0
Numerical setting	Time step [s]	$5\text{x}10^{-10}$
	Macro particle size	$4\text{x}10^{7}$
	Mass ratio m_i/m_e	96.4
	Grid spacing [mm]	0.2

C. Efficiency Analysis

The details of the used efficiency analysis scheme follows the work of Brown.[14] Anode efficiency is calculated by excluding electron source such as hollow cathode and magnetic circuit input power in order to evaluate performance of a thruster-head design. Anode efficiency is a function of thrust, mass flow rate and discharge power. It can also be written in terms of energy efficiency, propellant efficiency, and beam efficiency as:

$$\eta_A = \frac{F^2}{2\dot{m}P_d} = \eta_E \Phi_P \Psi_B \tag{1}$$

Where, F is thrust, $\dot{m}$ is anode mass flow rate, P_d is discharge power, η_E is energy utilization efficiency, Φ_P is propellant utilization efficiency, and Ψ_B is beam efficiency, η_E is defined as:

$$\eta_E = \eta_V \eta_C = \frac{P_{jet}}{P_d} = \frac{\frac{1}{2}\dot{m}_T \langle \overline{v^2} \rangle_m}{V_d I_d} \tag{2}$$

Where, η_V is voltage utilization efficiency, η_C is current utilization efficiency, P_{jet} is jet power responsible for the energy of neutral propellant, $\langle \overline{v^2} \rangle_m$ is mass weighted average of square of velocity, V_d is discharge voltage, and I_d is discharge current.

$$\Phi_p = \frac{\langle \overline{v} \rangle_m{}^2}{\langle \overline{v^2} \rangle_m} = \Phi_q \Phi_m \Phi_{N-G} = \left(\frac{\langle \overline{v_i} \rangle_m{}^2}{\langle \overline{v_i{}^2} \rangle_m}\right)\left(\frac{\dot{m}_i}{\dot{m}}\right)\left(1 + 2y_0 \frac{(1-\Phi_m)}{\Phi_m \sqrt{Q\Phi_q}}\right) \tag{3}$$

Where, $\langle \overline{v} \rangle_m$ is mass weighted average velocity, Φ_q is charge utilization efficiency, Φ_m is mass utilization efficiency, and Φ_{N-G} is neutral gain, which is always higher than unity, $\langle \overline{v_i} \rangle_m$ is mass weighted average ion velocity, $\langle \overline{v_i{}^2} \rangle_m$ is mass weighted average of square of ion velocity, $\dot{m}_i$ is ion mass flow rate, y_0 is normalized speed ratio for neutrals, and Q is average ion charge.

$$\Psi_B = \left(\frac{F}{\dot{m}\langle \overline{v} \rangle_m}\right)^2 \tag{4}$$

Table 2 summarizes definitions of these efficiency analysis scheme.

Table 2. Description of efficiency breakdown components.

Efficiency	Symbol	Description
Voltage utilization	η_V	Explains amount of the potential energy which is converted to kinetic energy
Current utilization	η_C	Compares thrust-generating ion current to discharge current
Mass utilization	Φ_m	Shows to what extent neutral propellant gets ionized and contributes to thrust
Charge utilization	Φ_q	Measures overall charge state of the beam ions
Neutral gain	Φ_{N-G}	Characterizes the effect of unionized neutral propellant on the velocity distribution function (VDF)
Beam utilization	Ψ_B	Used to analyses plume focusing by ion acceleration direction that are not parallel to the thruster centerline

D. Uncertainties Investigated in This Study

Sources of errors may be divided into two subcategories: 1) Discretization errors due to numerical computation, 2) Errors due to uncertainties in code input parameters related to physical phenomena, which will be named physical uncertainties hereafter. Errors in numerical calculations come from approximations to solve partial differential equations and physical recovery models such as macro particle number and mass ratio. Physical uncertainties come from lack of experiments to measure certain parameters such as thermal accommodation coefficient, and lack of knowledge to model complex phenomena such as Bohm diffusion. The scope of this paper is the sensitivity analysis of physical uncertainties, though the consideration about numerical errors will be discussed in section III.F.

Table 3 summarizes the uncertainties investigated in this study. The nominal value of each uncertainties and its range was presumed according to experimental evidence as follows. Note that the range of the parameters was taken as wide as possible to present a conservative confidence range of the simulation.

In the fully kinetic code, there are two kinds of thermal accommodation coefficients: ion energy accommodation named E_{co} in this study, and neutral energy accommodation, T_{co}. Velocity components of the ions hitting the discharge chamber walls are assigned according to a half-range Maxwellian distribution. Velocity components of the neutrals reaching the walls are assigned according to either a diffuse reflection or a specular reflection, which is decided randomly. At the anode region, both ions and neutrals' velocity components are assigned according to a half-range Maxwellian. As for the momentum accommodation, ions are fully accommodated, whereas T_{co} is also used as transverse momentum accommodation coefficient (TMAC) for the neutral particles. Experimental work of V. Kim et al.[15] suggests a Xenon accommodation coefficient on Boron Nitride between 0.6 and 0.8 for ion energies between 100 and 400 eV. Therefore, an accommodation coefficient of 0.5 was chosen as the lower bound, and of 1.0 as the upper bound.

The perpendicular component of the classical diffusion coefficient scales with $1/B^2$, and it is given as:

$$D_{\perp} = \frac{D}{1 + \omega_c^2 \tau^2} \tag{5}$$

Where ω_c is electron plasma frequency, and τ is average collision time.

In plasma devices like Hall thrusters, electron transport is found to be more than the classic diffusion coefficient predicts. This excessive electron transport was first observed by David J. Bohm in 1949.[16] Dr. Bohm described an empirical coefficient to scale this excessive electron diffusion plasma across magnetic fields. Although almost seven decades passed since its observation still there does not exist a physical model to incorporate this anomalous electron diffusion into numerical simulations. Hence, it is a common practice in fully kinetic simulations of Hall thrusters that a Bohm diffusion coefficient of 1/16 is mostly used to tune up the simulation results. However, 1/16 is not a certain value and the coefficient of 1/16 may be used within an uncertainty factor of 2 or 3 according to plasma instability.

$$D_B = \frac{1}{16} \frac{K_B T}{qB} \tag{6}$$

Where K_B is the Boltzmann constant, B is the magnetic field strength, T is the temperature, and q is the unit charge. As a simulation nominal, a Bohm diffusion coefficient of 1/16 is used. To obtain an error bar for physical uncertainties arising from anomalous cross-field electron diffusion, a Bohm diffusion coefficient of 1/8 was employed as the upper bound. Only classical diffusion, that is to say no Bohm diffusion, was assumed as the lower bound.

The voltage utilization efficiency is defined as the ratio of beam voltage to discharge voltage as $\eta_V = V_b/V_d$. As for the beam voltage, it is defined as $V_b = V_d - V_c$, where V_c is the cathode coupling voltage. Large cathode coupling voltage is undesirable since it decreases the available potential energy that ions convert into kinetic energy and thus generate thrust. Cathode coupling voltage in a Hall thruster is usually around 10-30 V. To quantify its effect, a maximum V_c of 30 V was assumed according to the measurement result of thrusters operating at similar conditions,[8] and the applied anode potential was simply reduced by V_c.

In the fully kinetic code, electrons are injected by providing charge neutrality at each plume boundary cells. Note that this electron injection current is not the same as the cathode electron emission current because the cathode is excluded from the computational domain. As simulation nominal, electron injection current is 2 A, which equals to the double of xenon propellant equivalent current. To quantify its effect, 1 A and 3 A were selected as the lower and upper bounds respectively.

Many studies in the literature[9, 10] conclude that vacuum chamber background pressure has remarkable influence on Hall thruster plasma properties, and performance parameters especially for high power applications.[17] Thus, it is necessary to correct experimental results to predict thruster's in-space performance. The background pressure effect may be considered as an experimental measurement error since it yields to increase in thrust and efficiency. During the experiments of the UT-62 thruster, the background pressure was kept lower than 3.7x10^{-3} Pa (~2.8x10^{-5} Torr) against 1.36 mg/s (+ 0.27 mg/s cathode) xenon mass flow rate.[13] This pressure was gauged at a point far away from the thruster exit, so it may be assumed that the pressure near the thruster exit plume region would be much higher. Therefore, the background pressure upper bound was chosen as 5x10^{-5} Torr.

Finally, the overall uncertainty integrated from all the individual sources of uncertainties can be derived as follows. Assuming the independency of each uncertainties of simulation result caused by individual source, an arbitrary overall uncertainty δq can be written as follows according to the uncertainty propagation rule:

$$\delta q = \sqrt{\left(\frac{\partial q}{\partial x}\delta x\right)^2 + \left(\frac{\partial q}{\partial y}\delta y\right)^2 + \cdots} \tag{7}$$

Where, $x, y, \ldots$ are individual source of uncertainties. Now if we approximate the partial derivative as $\partial q/\partial x = (\delta q)_x/\delta x$, the overall uncertainty reduces to the simple root sum square of the individual uncertainties$(\delta q)_x, (\delta q)_y$. This simplified method was applied to the simulation result substituting the difference from the nominal case into$(\delta q)_x, (\delta q)_y, etc.$ Note the "plus" and "minus" of the overall uncertainty was calculated separately according to Eq. 7.

Table 3. Investigated uncertainties.

Uncertainty	Nominal value	Maximum value	Minimum value
Ion accommodation coefficient	0.9	1.0	0.5
Neutral accommodation coefficient	0.9	1.0	0.5
Anode temperature [K]	500	900	500
Wall temperature [K]	700	900	500
Bohm diffusion coefficient	1/16	1/8	0
Cathode coupling [V]	0	30	0
Electron current [Aeq]	2	3	1
Background pressure [Torr]	0	5×10^{-5}	-

III. Results & Discussion

Figure 1 presents the overview of the simulation result of one-at-a-time sensitivity analysis illustrating the simulated and measured thrust and discharge current. At a glance, it was shown that the uncertainty of neutral flow (thermal accommodation coefficient & anode/wall temperature) and Bohm diffusion coefficient were by far the most influential. The confidence range of the fully kinetic code reasonably covers the experimental result, thought the overall uncertainty was considerably large (+15%-16% for thrust and +14%-19% for discharge current). Therefore, it was suggested that narrowing the confidence range of Bohm diffusion model and parameters related to neutral flow can effectively contribute to increasing the accuracy of fully kinetic simulation. It is found that the uncertainties originates the neutral flow (thermal accommodating coefficient and anode/wall temperature) was found to be as influential as the Bohm diffusion coefficient, though less attention was paid for them so far. This was one of the most important findings of this study. The details of the individual uncertainties are to be discussed in following sections.

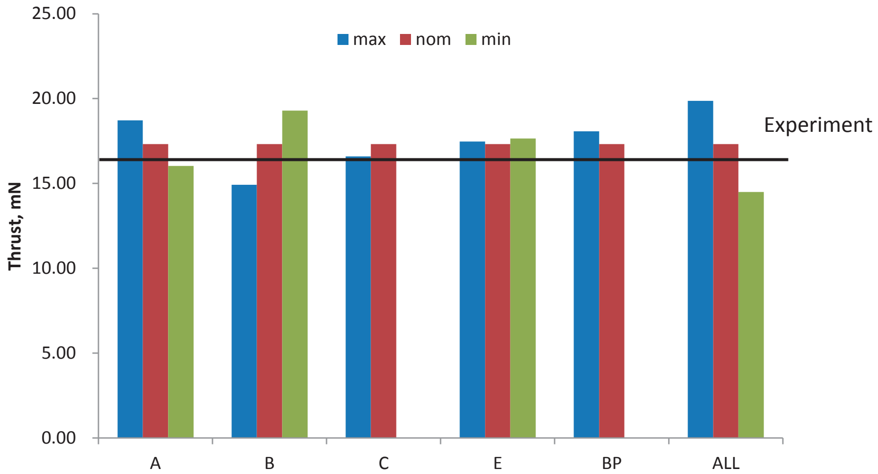

(a) Thrust

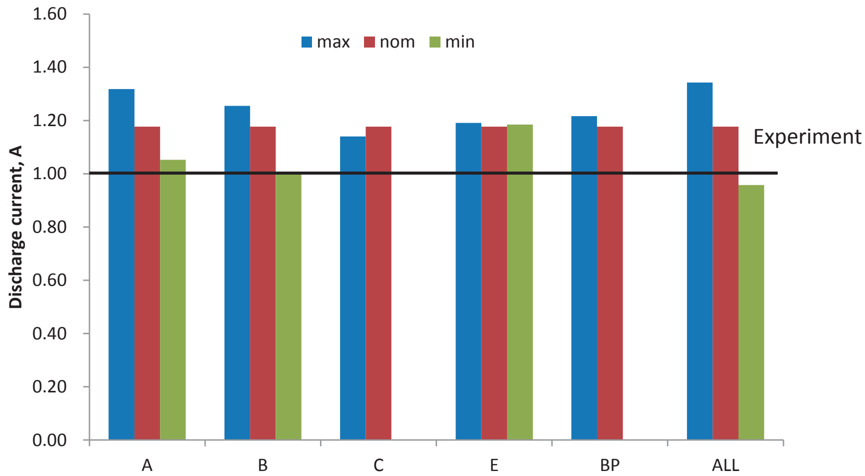

(b) Discharge current

Figure 1. Simulation result of thrust and discharge current one-at-a-time sensitivity analysis. *A: Thermal accommodation coefficient & anode/wall temperature, B: Bohm diffusion coefficient, C: Cathode coupling voltage, E: Electron injection current, BP: Background pressure effect, ALL: Overall uncertainty. Note the nom: nominal condition is displaying the same result for all of the cases.*

E. Thermal Accommodation Coefficient & Anode/Wall Temperature

In Table 4, case A_{nom} shows simulation nominal configuration of thermal accommodation coefficient and anode/wall temperature. From our previous paper,[18] it was concluded that these four uncertainties related to neutral flow can be investigated all together due to the monotonicity. Therefore, the case A_{max} and A_{min} was chosen to represents the upper bound and the lower bound. In addition, Figure 2 illustrates the simulated ion density of A_{max} and A_{min} case.

It may be seen from Table 4 that any change in thermal accommodation coefficient and temperature mostly affects neutral current (In), which is defined as amount of neutral particles leaving the thruster exit without getting ionized. When thermal accommodation coefficient is increased or temperature is decreased, kinetic energy or mean velocity of the neutrals is decreased. When neutrals have lower mean velocity, total time they stay in discharge chamber is increased yielding to higher electron-neutral collision probability/electron mobility, and thus higher ion density, which may be seen in Figure 2.

Mass utilization efficiency, beam efficiency, and voltage utilization efficiency are the efficiencies mostly affected by for the accommodation coefficient and anode/wall temperature. It is clear that neutrals having lower mean velocities will improve mass utilization efficiency because neutrals will have more chance to collide with electrons gyrating around magnetic field lines in discharge chamber. Beam efficiency tends to increase considerably towards the lower bound. An explanation may be that higher electron-neutral collision probability will move ionization region upstream, and thus more ions will collide with neutrals and electrons gaining velocity components in directions perpendicular to thruster axis. Although current utilization efficiency does not change significantly, equipotential lines move slightly downstream towards the upper bound and increasing the voltage utilization efficiency. As for charge utilization efficiency (Φ_q) and neutral-gain utilization efficiency ($\Phi_{N\text{-}G}$), they were not shown in this paper because there was not any significant change. However, it may be expected that $\Phi_{N\text{-}G}$ will increase slightly at higher anode/wall temperatures.

Regarding the wall erosion, higher accommodation coefficients and lower temperatures increase ion density and ion kinetic energy leading more ions to flux to the wall. The more ions with higher mean kinetic energies hit against discharge chamber walls the more atoms are ejected from the wall, and thus higher erosion rates or mass losses.

Table 4. Simulation input and output parameters for the accommodation coefficient & anode/wall temperature physical uncertainty.

Case			A_{nom}	A_{max}	A_{min}
Sensitivity (Input) Parameters	Acom. Coef.	T_{co}	0.9	1.0	0.5
	Acom. Coef.	E_{co}	0.9	1.0	0.5
	Anode Temp.	T_{anode}[K]	500	500	900
	Wall Temp.	T_{wall}[K]	700	500	900
Output Parameters (Numerical Simulation Results)	Thrust	F[mN]	17.3	18.7	16.0
	Discharge current	I_d[A]	1.18	1.32	1.05
	Singly charged ion current	I_{b1}[A]	0.78	0.87	0.71
	Doubly charged ion current	I_{b2}[A]	0.11	0.13	0.10
	Neutral current	I_n[A]	0.16	0.05	0.25
	Oscillation Amplitude	Δ	0.02	0.02	0.04
	Anode efficiency	η_A[%]	31.4	32.9	29.5
	Energy efficiency	η_E[%]	57	58	55
	Voltage utilization efficiency	η_V[%]	75	77	71
	Current utilization efficiency	η_C[%]	76	76	77
	Propellant efficiency	Φ_P[%]	84	94	76
	Mass utilization efficiency	Φ_m[%]	84	95	75
	Beam efficiency	Ψ_B[%]	65	60	71
	Inner Wall Erosion Rate	Total [mm^3/h]	1.5	1.4	1.0
		Max [mm/kh]	11.5	10.1	8.1
	Outer Wall Erosion Rate	Total [mm^3/h]	7.0	6.9	6.9
		Max [mm/kh]	23.2	26.2	18.4

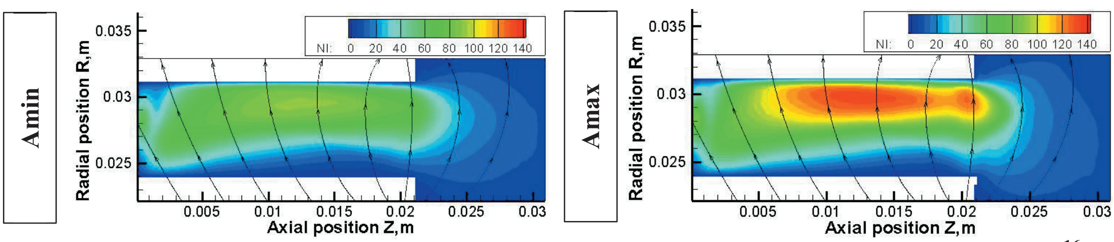

Figure 2: Lower bound (A_{min}) and upper bound (A_{max}) plasma ion density distribution (NI, (10^{16} m^{-3}) for the accommodation coefficient & anode/wall temperature physical uncertainty.

F. Bohm Diffusion Coefficient

Table 5 lists simulation input and output parameters for the Bohm diffusion physical uncertainty. As it may be expected, thruster performance deteriorates with higher cross-field electron diffusion mainly because of increased discharge current, neutral current and doubly-charged ion current. Improved voltage utilization towards the upper bound may be attributed to higher electron-neutral collision probability, which moves ionization region upstream and lead ions to be created with more potential energy to turn into kinetic energy. Beam efficiency is an indicator of plume divergence, and it may be said that plume divergence is the main factor for changes in the anode efficiency. Current utilization efficiency is also another major contributor to anode efficiency. It would not be wrong to say that charge utilization efficiency is correlated to doubly-charged ion current. Therefore, any increase in doubly-charged ion current causes current utilization to lessen. Regarding the wall erosion, it gets increased since more electrons pass through the radial magnetic field lines and let ions to be born in more potential energy rich region, closer to the anode, and have more kinetic energies in case of a higher Bohm diffusion coefficient.

Table 5. Simulation input and output parameters for the Bohm diffusion physical uncertainty.

Case			B_{nom}	B_{max}	B_{min}
Sensitivity (Input) Parameters	Bohm diffusion coefficient	**Bohm**	1/16	1/8	0
Output Parameters (Numerical Simulation Results)	Thrust	**F[mN]**	17.3	14.9	19.3
	Discharge current	$\mathbf{I_d}$**[A]**	1.18	1.26	1.00
	Singly charged ion current	$\mathbf{I_{b1}}$**[A]**	0.78	0.76	0.79
	Doubly charged ion current	$\mathbf{I_{b2}}$**[A]**	0.11	0.12	0.10
	Neutral current	$\mathbf{I_n}$**[A]**	0.16	0.18	0.16
	Oscillation Amplitude	$\mathbf{\Delta}$	0.02	0.02	0.03
	Anode efficiency	η_A**[%]**	31.4	21.7	45.4
	Energy efficiency	η_E**[%]**	57	55	63
	Voltage utilization efficiency	η_V**[%]**	75	79	71
	Current utilization efficiency	η_C**[%]**	76	70	89
	Propellant efficiency	Φ_P**[%]**	84	82	84
	Mass utilization efficiency	Φ_m**[%]**	84	82	84
	Beam efficiency	Ψ_B**[%]**	65	48	86
	Inner Wall Erosion Rate	**Total [mm^3/h]**	1.5	1.8	0.3
		Max [mm/kh]	11.5	13.5	2.0
	Outer Wall Erosion Rate	**Total [mm^3/h]**	7.0	6.5	5.5
		Max [mm/kh]	23.2	25.9	14.6

G. Cathode Coupling Voltage

Table 6 lists simulation input and output parameters for the cathode coupling physical uncertainty. Although cathode coupling effects tends to decrease thrust and efficiency and it has quite small effect. For a singly charged propellant the thrust is defined as:

$$T = \sqrt{\frac{2M}{q}}\, I_b \sqrt{V_b} \tag{8}$$

Where M is ion mass, q is the unit charge, I_b is beam current, and V_b is average beam potential. Equation shows that thrust is proportional to square root of beam voltage. So, thrust is expected to decrease about 5% for the given 30 V cathode coupling voltage. It may be deducted from Table 7 that cathode coupling effect can be treated by simply decreasing the applied potential on the anode, since both thrust and power decreased just as the theoretical prediction. As a matter of course, voltage utilization efficiency decreases. Mass utilization efficiency slightly decreases as well. A possible reason to that may be reduced electron-neutral collisions. Furthermore, an increase of 7% in plume divergence is noteworthy. Regarding the wall erosion, reduced voltage utilization naturally decreases erosion rates in the discharge chamber walls.

Table 6. Simulation input and output parameters for the cathode coupling physical uncertainty.

	Case		C_{nom}	C_{max}
Sensitivity (Input) Parameters	Cathode coupling voltage	**V_c[V]**	0	30
Output Parameters (Numerical Simulation Results)	Thrust	**F[mN]**	17.3	16.6
	Discharge current	**I_d[A]**	1.18	1.14
	Singly charged ion current	**I_{b1}[A]**	0.78	0.78
	Doubly charged ion current	**I_{b2}[A]**	0.11	0.11
	Neutral current	**I_n[A]**	0.16	0.16
	Oscillation Amplitude	**Δ**	0.02	0.02
	Anode efficiency	**η_A[%]**	31.4	29.7
	Energy efficiency	**η_E[%]**	57	51
	Voltage utilization efficiency	**η_V[%]**	75	65
	Current utilization efficiency	**η_C[%]**	76	78
	Propellant efficiency	**Φ_P[%]**	84	84
	Mass utilization efficiency	**Φ_m[%]**	84	84
	Beam efficiency	**Ψ_B[%]**	65	69
	Inner Wall Erosion Rate	**Total [mm^3/h]**	1.5	0.9
		Max [mm/kh]	11.5	7.1
	Outer Wall Erosion Rate	**Total [mm^3/h]**	7.0	5.7
		Max [mm/kh]	23.2	17.4

H. Electron Injection Current

Table 7 lists simulation input and output parameters for the electron injection current physical uncertainty. In short, it may be concluded that electron injection current has insignificant effect. It is known for Hall thrusters from experiments that cathode current (electron emission current) can control the plasma flow and plume divergence.[19] It is plume divergence, which is mostly affected by the electron injection current. Besides, it might be expected that wall erosion would increase for a given higher electron injection current because of increased ionization rate.

Table 7. Simulation input and output parameters for the electron injection current physical uncertainty.

	Case		E_{nom}	E_{max}	E_{min}
Sensitivity (Input) Parameters	Electron injection current	**I_{dedt}[A]**	2	3	1
Output Parameters (Numerical Simulation Results)	Thrust	**F[mN]**	17.3	17.5	17.7
	Discharge current	**I_d[A]**	1.18	1.19	1.18
	Singly charged ion current	**I_{b1}[A]**	0.78	0.79	0.79
	Doubly charged ion current	**I_{b2}[A]**	0.11	0.11	0.11
	Neutral current	**I_n[A]**	0.16	0.15	0.16
	Oscillation Amplitude	**Δ**	0.02	0.02	0.02
	Anode efficiency	**η_A[%]**	31.4	31.4	32.2
	Energy efficiency	**η_E[%]**	57	57	57
	Voltage utilization efficiency	**η_V[%]**	75	76	75
	Current utilization efficiency	**η_C[%]**	76	76	76
	Propellant efficiency	**Φ_P[%]**	84	84	84
	Mass utilization efficiency	**Φ_m[%]**	84	84	84
	Beam efficiency	**Ψ_B[%]**	65	65	67
	Inner Wall Erosion Rate	**Total [mm^3/h]**	1.5	1.6	1.5
		Max [mm/kh]	11.5	12.5	11.8
	Outer Wall Erosion Rate	**Total [mm^3/h]**	7.0	7.2	6.9
		Max [mm/kh]	23.2	23.8	22.4

It was observed that physical uncertainty due to electron injection current is quite low. It should be noted that cathode's position also affects the thruster performance in addition to cathode coupling voltage and cathode electron emission rate. For instance, Jameson, K. K., et al.[19] showed for a 6 kW Hall thruster that total thruster efficiency was improved by 2-3% when utilizing the internal cathode instead of and external cathode. However, this was out of the scope of this paper and was not investigated.

I. Background Pressure Effect

To quantify the background pressure effect, xenon neutrals with thermalized velocity components are introduced into the calculation region. To inject neutrals into the, a predetermined background pressure value is compared to the pressures of the each plume boundary cells. Neutrals are injected from a cell provided that the pressure in that cell is lower than the background pressure such that the pressure difference will be zero. If the boundary cell pressure is equal or higher than the background pressure than no injection is done. Besides, it was assumed that only xenon gas exists in the vacuum chamber. Figure 3 illustrates a diagram of neutral gas injection into the calculation area. Figure 4 shows thruster performance at different background pressures. There was almost no change in the thruster performance that for background pressures lower than 5×10^{-6} Torr. This may be explained in that there are small numbers of neutral xenon macro particles getting injected from the plume boundary cells simply because the pressure of those cells is higher than 5×10^{-6} Torr.

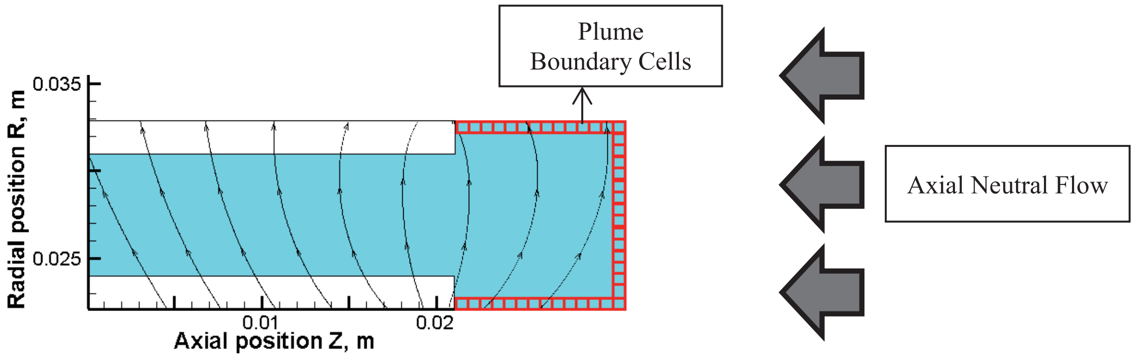

Figure 3: Diagram of neutral gas injection into the calculation area.

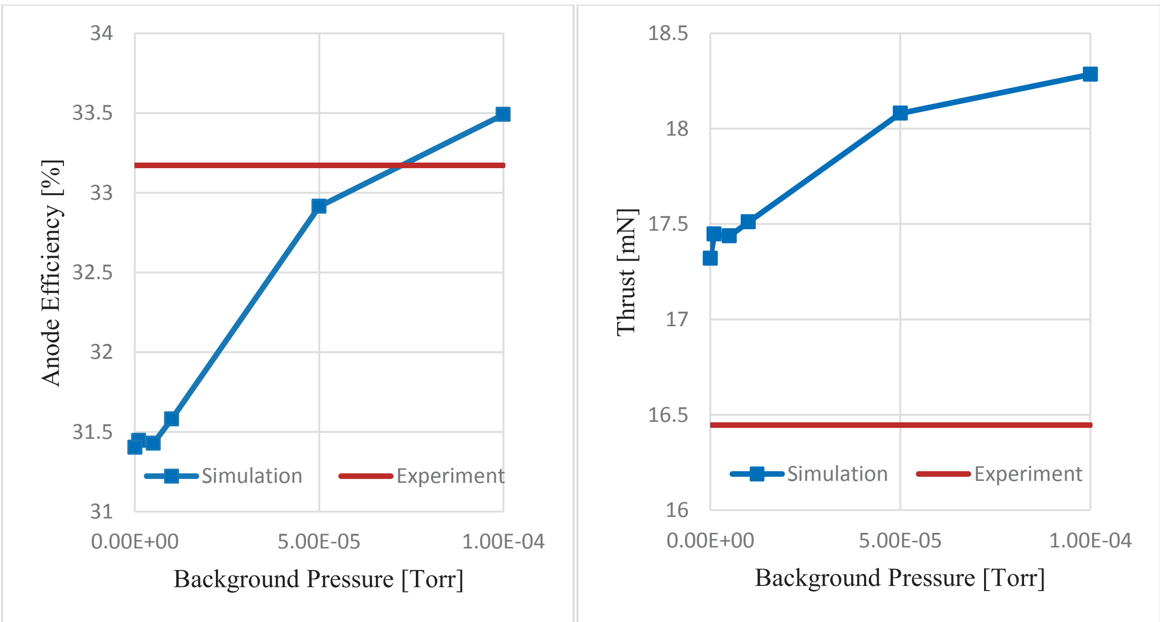

Figure 4: Anode efficiency and thrust results at different background pressures.

Table 8. Simulation input and output parameters for the background pressure uncertainty.

	Case		BP_{nom}	BP_{max}
Sensitivity (Input) Parameters	Background pressure	**Bp[Torr]**	0	$5x10^{-5}$
Output Parameters (Numerical Simulation Results)	Thrust	**F[mN]**	17.3	18.1
	Discharge current	**I_d[A]**	1.18	1.22
	Singly charged ion current	**I_{b1}[A]**	0.78	0.81
	Doubly charged ion current	**I_{b2}[A]**	0.11	0.12
	Neutral current	**I_n[A]**	0.16	0.21
	Oscillation Amplitude	**Δ**	0.02	0.02
	Anode efficiency	**η_A[%]**	31.4	32.9
	Energy efficiency	**η_E[%]**	57	56
	Voltage utilization efficiency	**η_V[%]**	75	74
	Current utilization efficiency	**η_C[%]**	76	77
	Propellant efficiency	**Φ_P[%]**	84	81
	Mass utilization efficiency	**Φ_m[%]**	84	81
	Beam efficiency	**Ψ_B[%]**	65	72
	Inner Wall Erosion Rate	**Total [mm^3/h]**	1.5	1.8
		Max [mm/kh]	11.5	14.2
	Outer Wall Erosion Rate	**Total [mm^3/h]**	7.0	7.5
		Max [mm/kh]	23.2	24.3

Table 8 lists simulation input and output parameters for the background pressure uncertainty. It is seen that anode efficiency and thrust get improved in case of existent background pressure. It may be said that the effect of the background pressure is about 5%. The interaction of background particles with the thruster plume decreases voltage utilization, mass utilization, and plume divergence. Reduction in plume divergence may be explained with boosted mean neutral velocities due to the background particles entering the thruster exit. Regarding the wall erosion, it increases with the background pressure. Positive change in the beam current may be given as a reason.

J. Discussion about Numerical Error

Investigation of the numerical errors was out of the scope of this study, though their importance is not negligible. Cho concluded in his previous paper[13] that $1x10^7$ macro particle number was a good trade-off between numerical errors and computational cost for this specific thruster. Table 9 shows that fully kinetic code may be assumed to be converged at a macro particle number of $1x10^7$.

Table 9. Fully kinetic code's convergence for macro particle number.

N_{macro}	F[mN]	I_d[A]	I_{b1}[A]	I_{b2}[A]	I_n[A]	Δ	η_A[%]
$4x10^7$	17.3	1.18	0.78	0.11	0.16	0.02	31.4
$3x10^7$	16.8	1.15	0.78	0.11	0.16	0.02	30.4
$2x10^7$	16.5	1.13	0.78	0.11	0.16	0.02	29.4
$1x10^7$	15.4	1.06	0.75	0.10	0.17	0.07	28.0
$7.5x10^6$	15.5	1.08	0.77	0.11	0.17	0.03	27.4
$5x10^6$	15.3	1.06	0.77	0.11	0.17	0.10	27.0
Experiment	16.4	1	-	-	-	0.16	33.2

However, using a lower macro particle number (N_{macro}) for parametric investigation demands higher amount of computation power and time; whereas, using a higher macro particle number increases numerical computation errors. To understand the relation between numerical computation errors and physical uncertainties, one of the physical uncertainty sources, a combination of thermal accommodation coefficient and anode/wall temperature, was examined with both a high ($4x10^7$) and a low ($1x10^7$) macro particle number. Simulation results related to the accommodation coefficient & anode/wall temperature physical uncertainty for $4x10^7$ and $1x10^7$ macro particle numbers were given in Table 10. It was suggested that even though the numerical computation error gets higher for a higher macro particle number, the fully kinetic code's response to physical uncertainty at both macro particle numbers is quite similar. It may be presumed that the physical uncertainty sources and numerical computation errors work independently. Therefore, the high macro particle number ($4x10^7$) was preferred for the sake of calculation time.

Table 10. Simulation results related to the accommodation coefficient & anode/wall temperature physical uncertainty for $4x10^7$ and $4x10^7$ macro particle numbers.

Nmacro	F[mN]	I_d[A]	I_{b1}[A]	I_{b2}[A]	I_n[A]	η_A[%]
$4x10^7$ A_{min}	17.3	1.18	0.78	0.11	0.16	31.4
$4x10^7$ A_{max}	18.7	1.32	0.87	0.13	0.05	32.9
% Difference	8	12	12	15	-67	5
$1x10^7$ A_{min}	15.4	1.06	0.75	0.10	0.17	28.0
$1x10^7$ A_{max}	16.6	1.21	0.85	0.12	0.07	28.5
% Difference	8	14	14	18	-60	2

IV. Conclusion

A systematic one-at-a-time sensitivity analysis of model parameter uncertainties for a fully kinetic particle code was presented to achieve better prediction accuracy of Hall thruster simulation. The investigated model parameters includes thermal accommodation coefficient, anode/wall temperature, Bohm diffusion coefficient, electron injection current, cathode coupling voltage, and background pressure, which were essentially all of the model input parameters of the code. The impact of each source of uncertainty on the simulation result was quantified one-by-one on a presumed possible range. The range was taken as wide as possible to present a conservative estimation of the confidence range of the simulation result. The simulation was conducted for a laboratory model magnetic layer type Hall thruster developed in the University of Tokyo.

The results show an overall confidence range of +15%-16% for thrust and +14%-19% for discharge current relative to the model parameter uncertainties. This confidence range comprises the experimental result of thrust and discharge current, which reasonably accounts for the discrepancies between the measured and simulated results. Among the sources of uncertainties, Bohm diffusion coefficient and uncertainties related to the neutral flow (thermal accommodation coefficient and anode/wall temperature) were by far the most influential, whereas the impact of other uncertainties including electron injection current, cathode coupling voltage, and background pressure were minor. It was found that uncertainties related to the neutral flow had comparable influence as the Bohm diffusion, which suggested that accurately identifying not only Bohm diffusion coefficient but also thermal accommodation coefficient and anode/wall temperature is essential for accurate predictive modeling of Hall thrusters.

Acknowledgments

The authors acknowledge the University of Tokyo Komurasaki laboratory for providing the UT-62 thruster configuration and measurement results. B. Karadag thanks Japanese Ministry of Education, Culture, Sports, Science, and Technology (MEXT) for his scholarship.

References

[1]Zhurin, V. V., H. R. Kaufman, and R. S. Robinson, "Physics of closed drift thrusters," *Plasma Sources Science and Technology* 8.1 (1999): R1.

[2]Mikellides, I. G. et al., "Magnetic shielding of walls from the unmagnetized ion beam in a Hall thruster," *Appl. Phys. Lett.* 102, 023509 (2013).

[3]J. C. Adam, A. Heron and G. Laval, *Phys. Plasmas*, 11, 295 (2004). doi:10.1063/1.163290

[4]Fife, John Michael, Manuel Martinez-Sanchez, and James Szabo, "A numerical study of low-frequency discharge oscillations in Hall thrusters." *Proc. 33rd AIAA Joint Propulsion Conference*. No. 97-3051. 1997.

[5]Parra, F. I., et al., "A two-dimensional hybrid model of the Hall thruster discharge," *Journal of Applied Physics* 100.2 (2006): 023304.

[6]Hofer, Richard R., et al., "Heavy Particle Velocity and Electron Mobility Modeling in Hybrid-PIC Hall Thruster Simulations," *AIAA Paper* 4658 (2006): 9-12.

[7]Hofer, Richard R., et al, "Efficacy of Electron Mobility Models in Hybrid-PIC Hall Thruster Simulations," *AIAA Paper* 4924 (2008): 2008.

[8]Jameson, Kristina K., et al., "Cathode coupling in Hall thrusters," *30th International Electric Propulsion Conference*. 2007.

[9]Randolph, T., et al., "Facility Effects on Stationary Plasma Thruster Testing," 23rd *International Electric Propulsion Conference*. 1993.

[10]Kamhawi, Hani, et al., "Investigation of the Effects of Facility Background Pressure on the Performance and Voltage-Current Characteristics of the High Voltage Hall Accelerator," IEPC-2013-446, *33rd International Electric Propulsion Conference*, Washington, DC, 2013.

[11]Hora, Stephen C., "Aleatory and epistemic uncertainty in probability elicitation with an example from hazardous waste management," *Reliability Engineering & System Safety* 54.2 (1996): 217-223.

[12]Cho, S., Watanabe, H., et al., "Parametric Kinetic Simulation of an IHI High Specific Impulse SPT -Type Hall Thruster," *50th AIAA/ASME/SAE/ASEE Joint Propulsion Conference & Exhibit*, Cleveland, OH, AIAA Paper 2014-3426, July 2014.

[13]S. Cho, K. Komurasaki, and Y. Arakawa, *Physics of Plasmas* 20, 063501 (2013).

[14]Brown, D. L., "Investigation of Low Discharge Voltage Hall Thruster Characteristics and Evaluation of Loss Mechanisms," *Ph.D. Dissertation*, University of Michigan, 2009.

[15]V. Kim, A. Semenov, I. Shkarban, "Investigation of the Accelerated Ions Energy Accommodation Under Their Impingement with Solid Surfaces," *38th AIAA/ASME/SAE/ASEE Joint Propulsion Conference & Exhibit*, July 7-10 2002, Indianapolis, Indiana, AIAA 2002-4110.

[16]Bohm, D. (1949), "The characteristics of electrical discharges in magnetic fields," A. Guthrie and R. K. Wakerling (eds.), New York: McGraw-Hill.

[17]Byers, D. and Dankanich, J.W., "A Review of Facility Effects on Hall Effect Thrusters," IEPC 2009-076.

[18]Karadag, B., Cho, S., Funaki, I., "Numerical Investigation of Thermal Accommodation Coefficient and Temperature Sensitivity in a Hall Thruster," *Plasma Conference 2014*, Niigata, Japan, Nov. 18-21, 2014.

[19]Jameson, K. K., Goebel, D. M., Hofer, R. R., and Watkins, R. M., "Cathode Coupling in Hall Thrusters," Presented at *the 30th International Electric Propulsion Conference*, IEPC Paper 2007-278, Florence, Italy, Sept. 17-20, 2007.